

Supplementary Information

Optical tweezers assisted coupling of nematic droplets to gold nanoparticle cluster : Effect on whispering gallery modes

Sumant Pandey[†] and G V Pavan Kumar^{†,*}

[†]Department of Physics, Indian Institute of Science Education and Research Pune, Pune, Maharashtra, 411008, India

*Email: pavan@iiserpune.ac.in

Contents

- S1 Experimental Setup**
- S2 SEM image of a 100 nm Au nanoparticle and its cluster.**
- S3 WGMs enhanced with gold nanoparticle cluster having 100 nm Au NPs basic unit.**
- S4 Red-shift of WGM spectra coupled to gold nanoparticle cluster having 100 nm Au NPs basic unit.**
- S5 Reversibility of modes on decoupling from gold nanoparticle cluster having 100 nm Au NPs basic unit.**
- S6 Red-shift of WGM spectra coupled to gold nanoparticle cluster having 200 nm Au NPs basic unit of main article figure 3.**
- S7 Red-shift of WGM spectra coupled to gold nanoparticle cluster having 200 nm Au NPs basic unit**
- S8 WGMs enhanced with gold nanoparticle cluster having 200 nm Au NPs basic unit.**

- S9 Size of droplet with dropcasted gold nanoparticle cluster in dark field microscope with basic unit 400 nm Au nanoparticle**
- S10 WGMs enhanced with gold nanoparticle cluster having 400 nm Au NPs basic unit.**
- S11 Photobleaching of dye in single droplet under continuous laser trapping.**
- S12 Photobleaching of dye in multile droplet under continuous laser trapping.**
- S13 Characterisation of AuNPs with basic units of 100/200/400 nm with statistical data.**
- S14 Table of plasmonic tuning observed in solid versus liquid crystal microresonator.**

S1. Experimental Setup

In our experiments, the sample is placed on an upright optical microscope setup, and light emitted on WGM excitation from the nematic microdroplet, which was collected with a spectrometer, as shown in Figure S1.

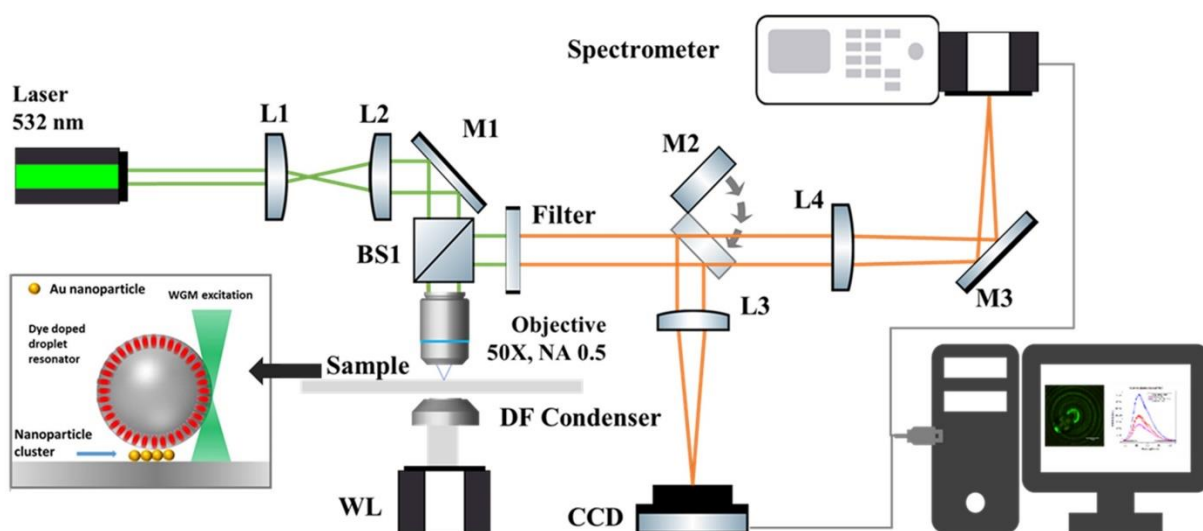


Figure S1: Schematic of the Upright microscope setup coupled with a dark-field condenser. A 532 nm continuous laser is used for optical excitation, and the experimental set up is composed of the white light source and lenses (L1, L2, L3, L4 and objective lens), mirrors (M1, M2, M3), 532 nm edge filter, CCD camera (Thorlabs digital camera) and spectrometer (iHR 320).

S2. SEM image of a 100 nm Au nanoparticle and its cluster

The gold nanoparticles suspended in ethanol solution were dropcasted on the glass substrate and it forms a cluster after evaporation of ethanol, as shown with a scale bar in figure S2. The inset shows the smallest gold nanoparticle with an average size of 100 nm.

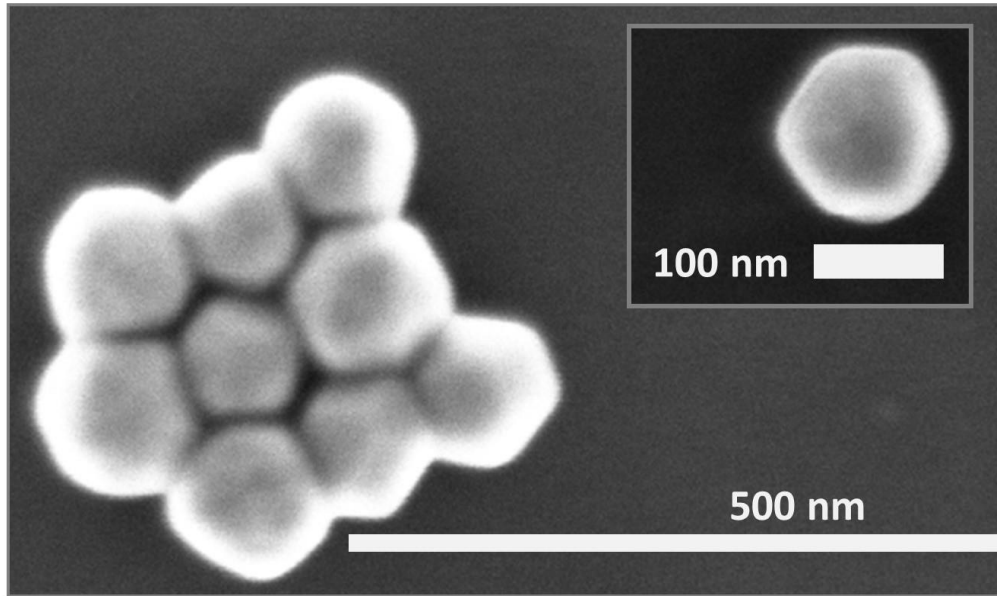


Figure S2: The drop-cast gold nanoparticles have a cluster with a scale bar shown. The inset shows the smallest gold nanoparticle with an average size of 100 nm.

S3. WGMs enhanced with gold nanoparticle cluster having 100 nm Au NPs basic unit.

The nematic microdroplet having diameter of 22 μm was excited with a 532 nm laser to obtain WGM spectra before coupling, and then the trapped microdroplet was parked on a gold nanoparticle cluster, and coupled WGM spectra are shown in Figure S3 in green and red colors, respectively. The coupling of plasmonic nanoparticles creates a locally enhanced electric field that significantly boosts the excitation and emission rate of dye molecules doped within the liquid crystal microdroplet [1, 6]. This results in a stronger fluorescence signal, which is efficiently emitted into the microdroplet resonator. The emitted light is then trapped and recirculated within the droplet through whispering gallery modes (WGMs), leading to fluorescence-enhanced WGM sustained spectra over it [1, 2]. The Q-factor of the highest intensity mode in the case of coupling gets slightly degraded compared to the case before coupling. Now the droplet was trapped and moved away from the plasmonic cluster, and the collected WGM spectra of the droplet are shown by blue color. The fluorescence intensity of WGM modes in the case of after coupling gets lowered in magnitude compared to the WGM spectra before coupling. It is shown that the intensity of modes also decreases due to the degradation of dye molecules due to the continuous trapping process.

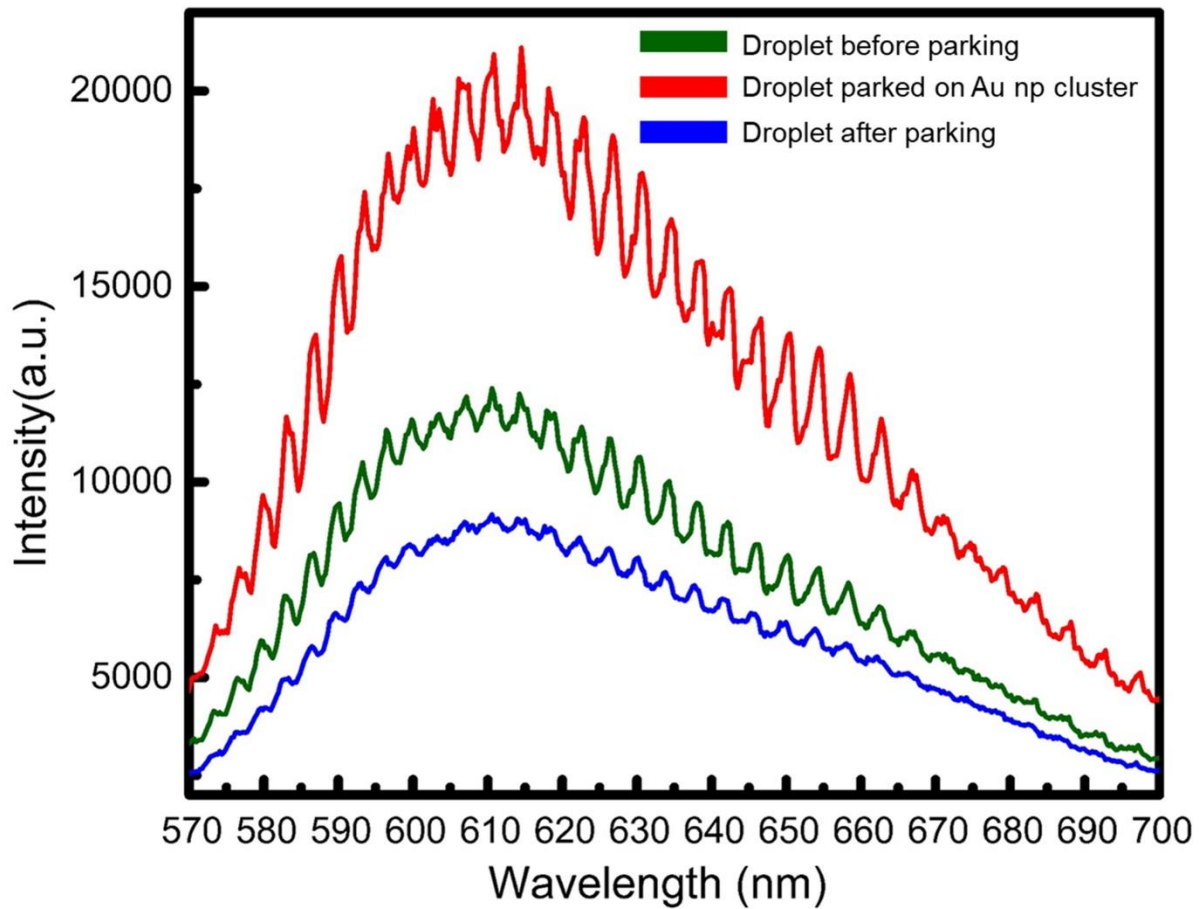


Figure S3: Whispering gallery mode (WGM) spectra of a dye-doped nematic microdroplet during coupling and decoupling with a gold nanoparticle cluster. The green color represents the WGM spectrum of the isolated droplet before coupling. The red color shows the WGM spectra when the droplet is coupled to the gold nanoparticle cluster. The blue color corresponds to the WGM spectra after coupling.

S4. Red-shift of WGM spectra coupled to gold nanoparticle cluster having 100 nm Au NPs basic unit.

Figure S4 shows the normalized WGM intensity spectrum of a 22 μm nematic droplet over the 570–700 nm range, captured before (green) and during (red) coupling with a gold nanoparticle cluster. To enhance the visibility of resonance features, the wavelength region between 590 and 650 nm is magnified in the central panel, indicates mode spacing and non overlapping highest intensity modes. A darker light-purple band within this central view is further highlighted with dotted lines and expanded in the rightmost panel, which focuses on the 600 to 625 nm range. A horizontal grey dotted line, drawn parallel to the wavelength axis, marks the peak normalized intensity for visual reference. This zoomed-in view clearly shows a redshift in the highest intensity

mode upon coupling. The highest normalized intensity before and during coupling touches the grey dotted line at different values of wavelength: 610.5 and 614.5 nm, respectively [3]. The Q factor of the highest intensity mode shows slight lowering in the case of coupling than before coupling. This confirms the coupling, showing that the fraction of WGM fields that are localized to the plasmonic cluster causes WGM resonance wavelength shifts. The distance between two consecutive modes that remains almost conserved is measured by the free spectral range (FSR); it is around 3.75 before coupling and during coupling. We can clearly see that there are very small peaks observed that evolve and have very low intensity that will be either of TE modes or TM modes of higher order [4].

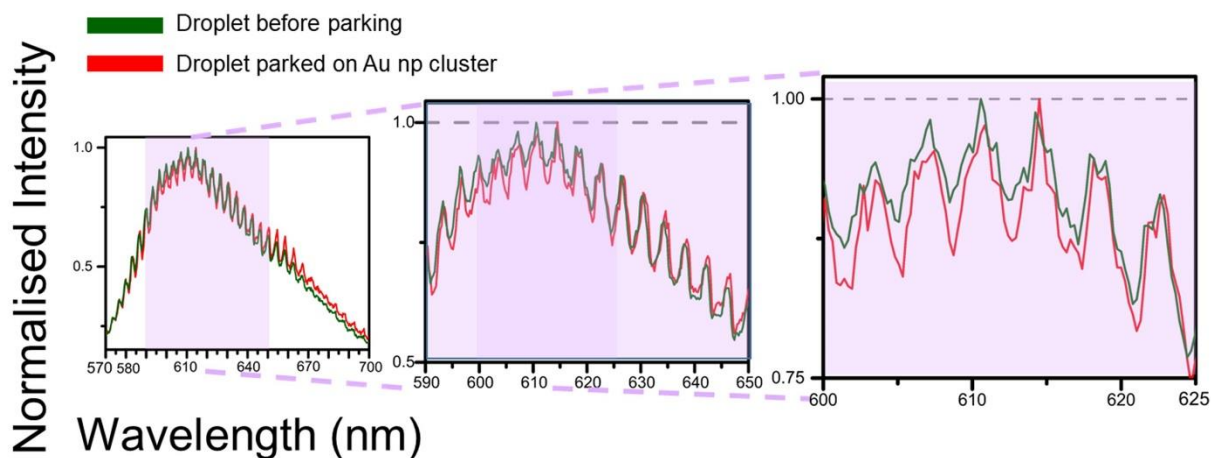


Figure S4: A normalized intensity versus wavelength plot of whispering-gallery modes (WGMs) of a dye-doped nematic microdroplet before (green) and during coupling (red) with a gold nanoparticle cluster. The left panel shows whispering-gallery modes over the broad fluorescence emission spectrum (570–700 nm) before and during coupling. The shaded light purple region is enlarged as indicated by dotted lines in the central panel (590–650 nm), highlighting mode spacing and the non-overlap of the highest intensity modes in decoupled and coupled states. The dark light-purple band in the central panel is further enlarged, as indicated by dotted lines, to show the regions of spectral magnification presented in the rightmost panel. This right panel zooms in on the 600–625 nm range, clearly showing the red shift of the highest intensity mode in the coupled state. A horizontal grey dotted line marks the peak normalized intensity to guide the eye in comparing the spectral shift of modes before and during coupling.

S5. Reversibility of modes on decoupling from gold nanoparticle clusters having 100 nm Au NPs basic unit.

Figure S5 presents the normalized intensity spectra of WGM modes from microdroplets before and after coupling with a gold nanoparticle cluster shown in green and blue, respectively, over the 570–700 nm range. To better visualize the resonance features, the light sky blue shaded region (590–650 nm) is enlarged in the central panel, highlighting mode spacing and overlap.

Within this range, a darker sky-blue section is further zoomed in and shown in the right most panel, focusing in the 600–620 nm spectral range. A horizontal dotted line, drawn parallel to the wavelength axis, marks the peak normalized intensity to guide comparison. The most intense modes before and after coupling align along this line, indicating strong spectral overlap and the reversible nature of the WGMs. Importantly, the linewidth ($\Delta\lambda$) of the resonance peak remains unchanged after coupling, suggesting that while the modes are highly sensitive to perturbations, the quality of the resonances is preserved. The Q-factor of the highest intensity mode shows a slight lowering in the case of after coupling as compared to the case of before coupling [5].

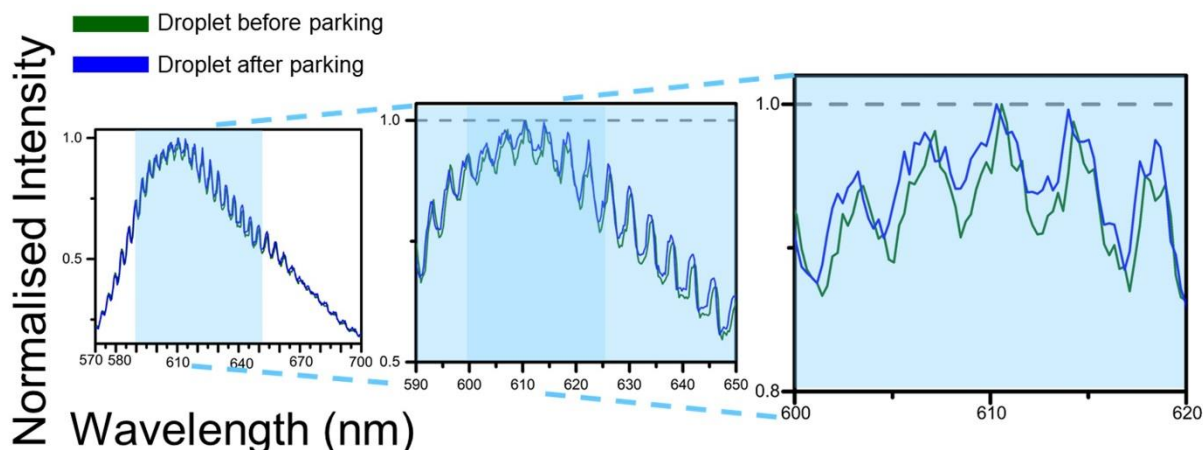


Figure S5: A normalized intensity versus wavelength plot of whispering-gallery modes (WGMs) of a dye-doped nematic microdroplet before (green) and after coupling (blue) with a gold nanoparticle cluster. The left panel shows whispering-gallery modes over the broad fluorescence emission spectrum (570–700 nm) before and after coupling. The shaded light sky-blue region is enlarged as indicated by dotted lines in the central panel (590–650 nm), highlighting mode spacing and the overlap of modes in decoupled states. The dark light sky-blue band in the central panel is further enlarged, as indicated by dotted lines, to show the regions of spectral magnification presented in the rightmost panel. This right panel zooms in on the 600–620 nm range, clearly showing overlapping of individual modes before and after coupling. A horizontal grey dotted line marks the peak normalized intensity to guide the eye in comparing the reversibility of the highest intensity modes in decoupled states.

S6. Red-shift of WGM spectra coupled to gold nanoparticle cluster having 200 nm Au NPs basic unit for main article Figure 3.

Figure S6 shows the normalized WGM intensity spectrum of a 24 μm droplet over the 570–700 nm range, captured before (green) and during (red) coupling with a gold nanoparticle cluster. To enhance the visibility of resonance features, the wavelength region between 590 and 650 nm is magnified in the central panel, indicating mode spacing and non-overlapping highest intensity modes. A darker light-purple band within this central view is further highlighted with dotted lines and expanded in the rightmost panel, which focuses on the 600 to 640 nm range. A horizontal

grey dotted line, drawn parallel to the wavelength axis, marks the peak normalised intensity for visual reference. This zoomed-in view clearly shows a redshift in the highest intensity mode upon coupling. The highest normalised intensity before and during coupling touches the grey dotted line at different values of wavelength: 608.2 and 609.5 nm, respectively [3]. The magnitude of redshift is small, and observed fluorescence enhancement without quenching is shown in the main article Figure 3 [6]. Apart from the red shift, the modes from 600 to 640 nm show splitting and thus the quality of the sharp modes during coupling gets degraded. This confirms the coupling, showing that the fraction of WGM fields that are localised to the plasmonic cluster gives WGM resonance wavelength shifts [3]. This coupling causes red shift, mode splitting and fluorescence enhancement together due to the plasmonic cluster of random size and shape.

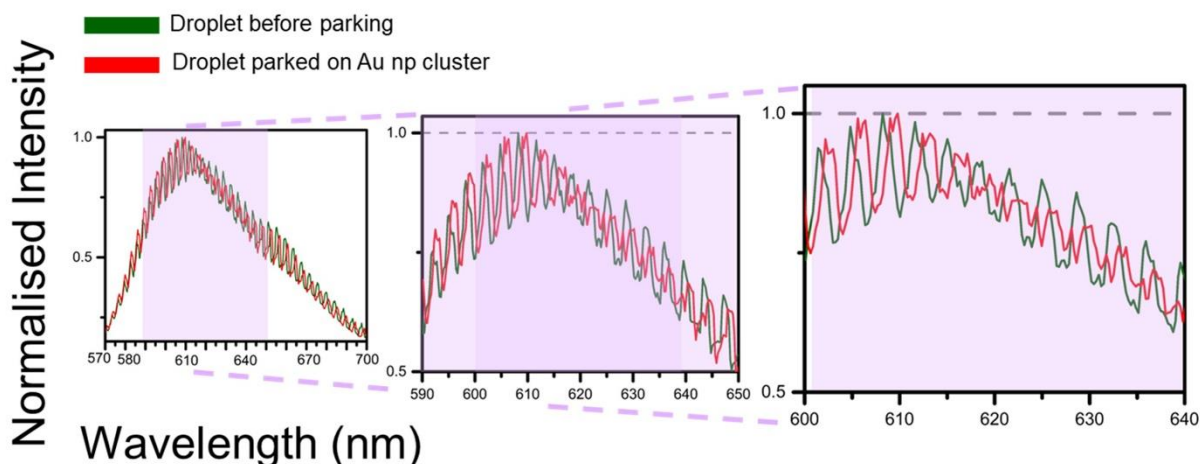


Figure S6: A normalized intensity versus wavelength plot of whispering-gallery modes (WGMs) of a dye-doped nematic microdroplet before (green) and during coupling (red) with a gold nanoparticle cluster. The left panel shows whispering-gallery modes over the broad fluorescence emission spectrum (570–700 nm) before and during coupling. The shaded light purple region is enlarged as indicated by dotted lines in the central panel (590–650 nm), highlighting mode spacing and the non-overlap of the highest intensity modes in decoupled and coupled states. The dark light-purple band in the central panel is further enlarged, as indicated by dotted lines, to show the regions of spectral magnification presented in the rightmost panel. This right panel zooms in on the 600–640 nm range, clearly showing the red shift of the highest intensity mode in the coupled state. A horizontal grey dotted line marks the peak normalized intensity to guide the eye in comparing the spectral shift of modes before and during coupling.

S7. Red-shift of WGM spectra coupled to gold nanoparticle cluster having 200 nm Au NPs basic unit.

To verify coupling we once again trapped the same 24 μm droplet and moved the mechanical stage to a location where a new gold nanoparticle cluster of different size dropcasted and was far from the previous parking location. The spectra were recorded by first exciting microdroplet

with a laser and then placing it onto a gold nanoparticle cluster. Figure S7 shows the normalized WGM intensity spectrum of a 24 μm droplet over the 570–700 nm range, captured before (green) and during (red) coupling with a gold nanoparticle cluster. To enhance the visibility of resonance features, the wavelength region between 590 and 650 nm is magnified in the central panel, indicates mode spacing and non overlapping highest intensity modes. A darker light-purple band within this central view is further highlighted with dotted lines and expanded in the rightmost panel, which focuses on the 600 to 620 nm range. A horizontal grey dotted line, drawn parallel to the wavelength axis, marks the peak normalized intensity for visual reference. This zoomed-in view clearly shows a redshift in the highest intensity mode upon coupling. The highest normalized intensity before and during coupling touches the grey dotted line at different values of wavelength indicating a shift of roughly 5.5 nm [3]. The distance between two consecutive modes that remains almost conserved is measured by the free spectral range (FSR); it is around 3.55 before coupling and during coupling. The observed redshift magnitude is above the free spectral range of WGM. We can clearly see that there are very small peaks observed that evolve and have very low intensity that will be of TE modes or TM modes of higher order [4].

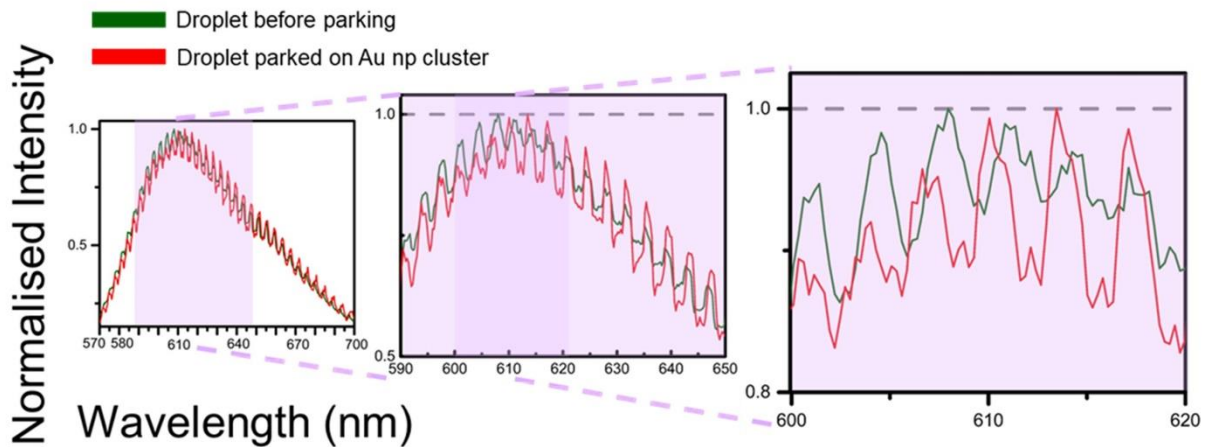


Figure S7: A normalized intensity versus wavelength plot of whispering-gallery modes (WGMs) of a dye-doped nematic microdroplet before (green) and during coupling (red) with a gold nanoparticle cluster. The left panel shows whispering-gallery modes over the broad fluorescence emission spectrum (570–700 nm) before and during coupling. The shaded light purple region is enlarged as indicated by dotted lines in the central panel (590–650 nm), highlighting mode spacing and the non-overlap of the highest intensity modes in decoupled and coupled states. The dark light-purple band in the central panel is further enlarged, as indicated by dotted lines, to show the regions of spectral magnification presented in the rightmost panel. This right panel zooms in on the 600–620 nm range, clearly showing the red shift of the highest intensity mode in the coupled state. A horizontal grey dotted line marks the peak normalized intensity to guide the eye in comparing the spectral shift of modes before and during coupling.

S8. WGMs enhanced with gold nanoparticle cluster having 200 nm Au NPs basic unit.

The same 24 μm droplet was excited with a green laser to obtain WGM spectra before coupling, and then, on suitable parking, coupled WGM spectra were shown in Figure S8 in green and red colors, respectively. The droplet emission spectra in the wavelength range of 570-700 nm reflect significant differences in intensity of fluorescence background sustained WGM spectra due to the presence of coupling with gold nanoparticle clusters as compared to WGM spectra of only microdroplets in the absence of coupling [1, 2]. We have found fluorescence enhancement for the small nanoparticle cluster in the same sample and observed fluorescence intensity increased by approximately 24 percent relative to before coupling value [1, 6]. The Q-factor of the highest intensity mode in the case of coupling gets slightly degraded compared to the case before coupling. Now the droplet was trapped and moved away from the gold nanoparticle cluster, and the collected WGM spectra of the droplet are shown by the blue color.

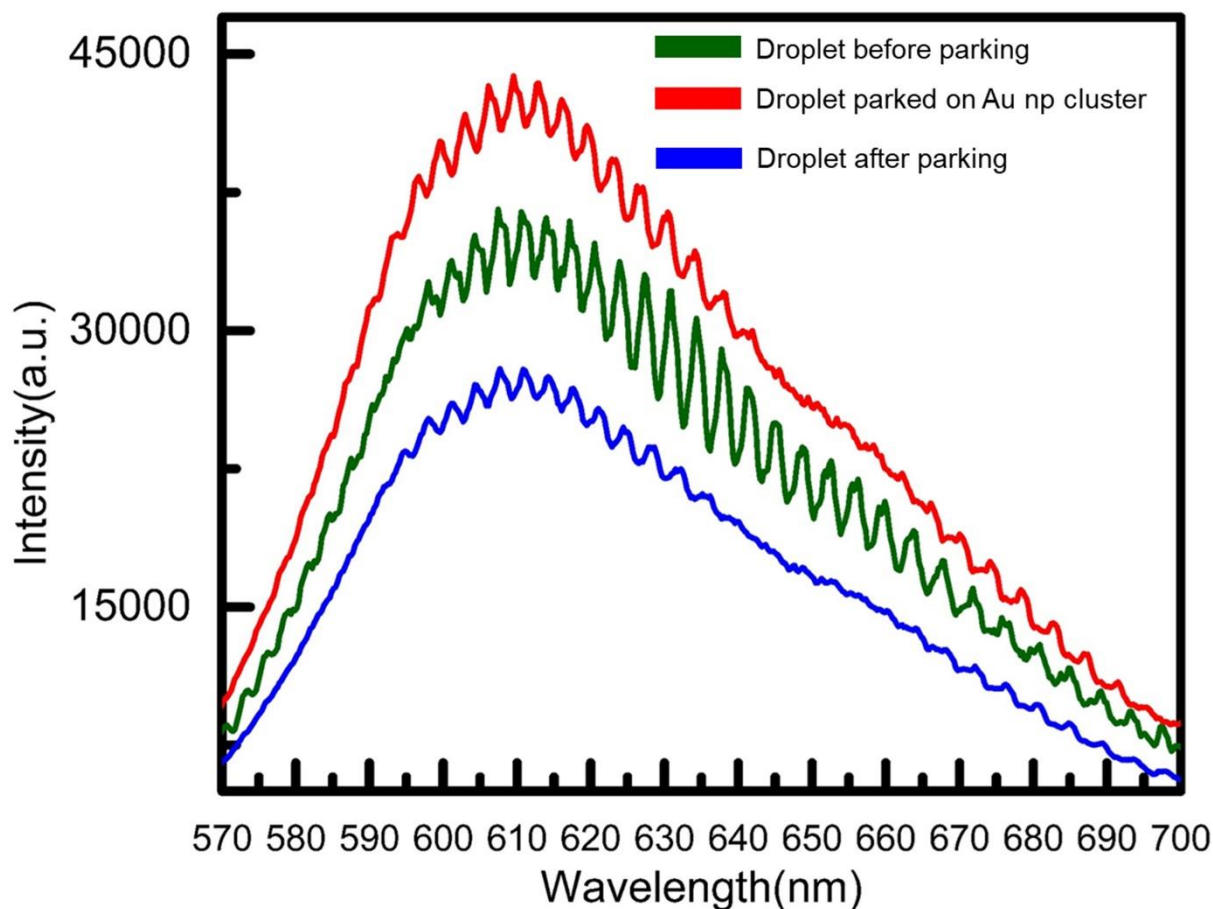


Figure S8: Whispering gallery mode (WGM) spectra of a dye-doped nematic microdroplet during coupling and decoupling with a gold nanoparticle cluster. The green color represents the WGM

spectrum of the isolated droplet before coupling. The red color shows the WGM spectra when the droplet is coupled to the gold nanoparticle cluster. The blue color corresponds to the WGM spectra after coupling.

S9. Size of droplet with dropcasted gold nanoparticle cluster in dark field microscope with basic unit 400 nm Au nanoparticle

To observe coupling effect, we have dropcasted gold nanoparticle which are visible as cluster. The image shown below these clusters and microdroplet in dark field with scale bar.

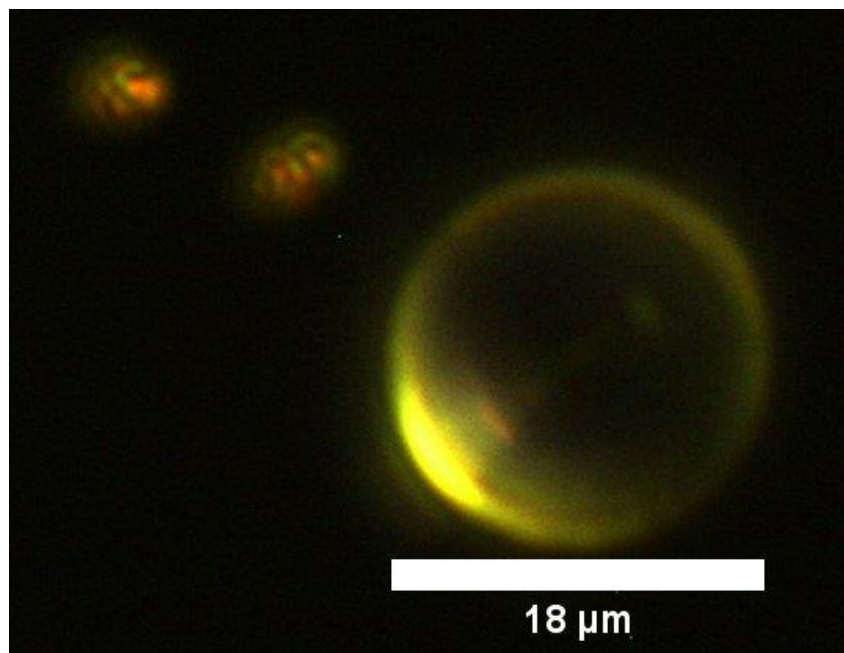


Figure S9: Size of droplet is 18 μm in dark field microscope and gold nanoparticle cluster in dark field microscope dropcasted with basic unit 400 nm Au nanoparticle.

S10. WGMs enhanced with gold nanoparticle cluster having 400 nm Au NPs basic unit.

A microdroplet of size 18 μm was excited with laser to obtain WGM spectra before coupling, and then, on suitable parking, coupled WGM spectra were shown in Figure S10 in green and red color respectively. The droplet emission spectra in the wavelength range of 570-700 nm reflect significant differences in intensity of fluorescence background sustained WGM spectra due to the presence of coupling with gold nanoparticle clusters as compared to WGM spectra of only microdroplet in the absence of coupling [1,2,6]. Now the droplet was trapped and moved away from the gold nanoparticle cluster, and the collected WGM spectra of the nematic microdroplet are shown by the blue color. The fluorescence intensity of WGM modes in the case of after

coupling is similar in magnitude compared to the WGM spectra before coupling. It is shown that the intensity of modes is comparable in magnitude in the continuous trapping process. The Q-factor of the microdroplet resonator in the case of after coupling remains the same as compared to the before coupling Q-factor. The free spectral range of a microdroplet in the case of coupling and decoupling remains same.

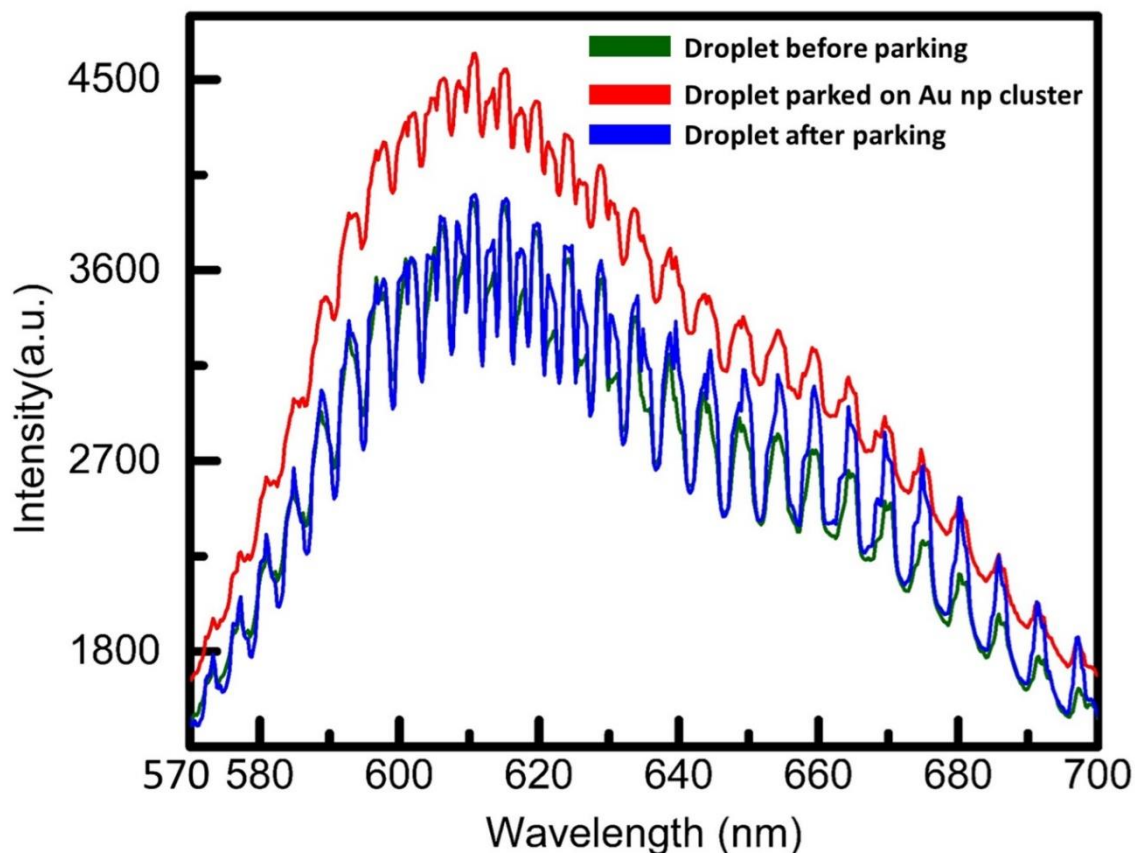


Figure S10: Whispering gallery mode (WGM) spectra of a dye-doped nematic microdroplet during coupling and decoupling with a gold nanoparticle cluster. The green color represents the WGM spectrum of the isolated droplet before coupling. The red color shows the WGM spectra when the droplet is coupled to the gold nanoparticle cluster. The blue color corresponds to the after coupling, where the droplet is once again isolated, showing the restoration of the WGM spectrum.

S11. Photobleaching of dye in single droplet under continuous laser trapping.

We performed control experiments in which dye-doped LC droplets were trapped by optical tweezers for the same duration as the coupling–decoupling experiments (<3 minutes per cycle) without the gold nanoparticle cluster. WGM spectra were collected at $t = 0, 2, 4,$ and 6 minutes.

The spectra showed overlapping WGM modes, confirming no change in droplet size, while a gradual decrease in fluorescence intensity was observed. This indicates that the observed fluorescence decay arises mainly from the thermal effects of laser irradiation rather than mechanical disturbance from the tweezers. Furthermore, we extended the trapping duration beyond the typical coupling–decoupling cycle (<3 minutes per cycle), demonstrating that our system remains stable and reliable for prolonged optical manipulation experiments.

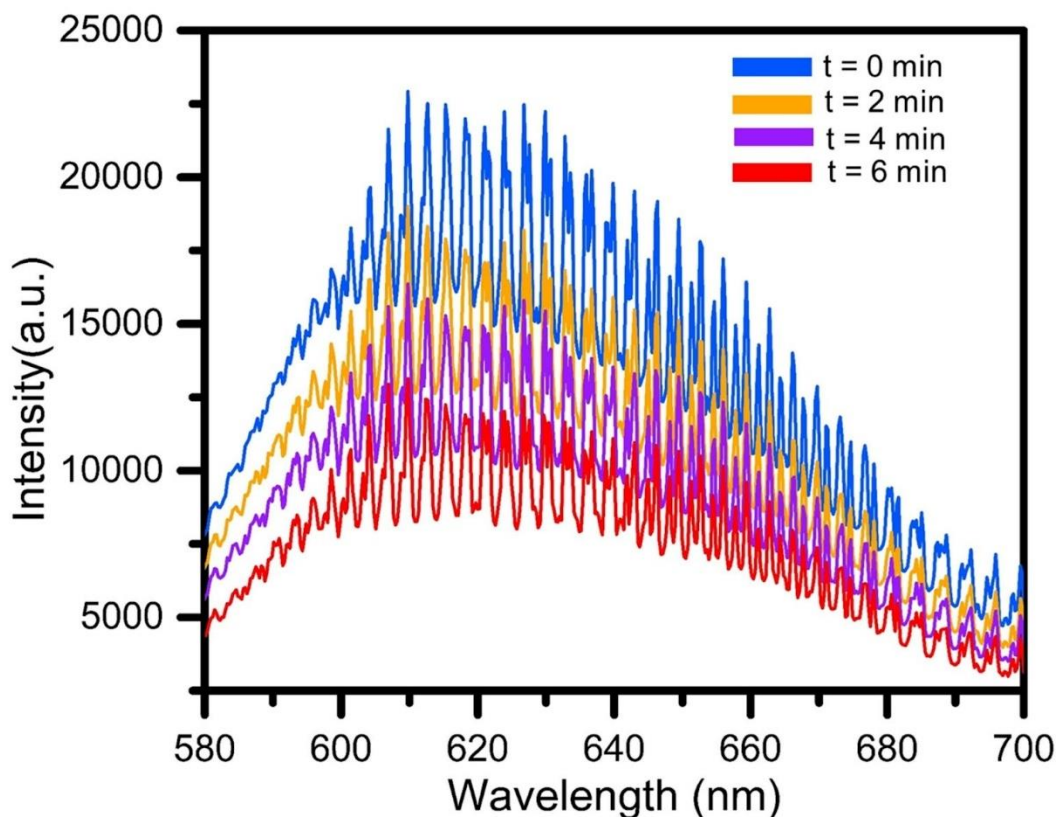


Figure 11. Time-dependent WGM spectra of a dye-doped liquid crystal microdroplet under optical trapping, recorded over the fluorescence background at different time intervals ($t = 0, 2, 4$, and 6 minutes). The measurements were performed to study the effect of prolonged laser trapping on the stability of the droplet's optical response.

S12. Photobleaching of dye in multiple droplet under continuous laser trapping.

We conducted additional control measurements on multiple dye-doped LC droplets prepared under identical conditions to assess dye photostability. In these tests, droplets were optically trapped for the same duration as the coupling–decoupling experiments (<3 minutes per cycle) without the gold nanoparticle cluster. WGM spectra collected at $t = 0, 2, 4$, and 6 minutes showed complete mode overlap, confirming no change in droplet size, while a gradual fluorescence

decrease was attributed primarily to thermal effects from laser exposure. Extended trapping beyond the typical cycle further confirmed droplet stability during prolonged manipulation.

Time-series spectra from droplets of different sizes (Droplet 1, 2 and 3) exhibited similar photobleaching trends with overlapping modes, verifying size stability throughout the experiment. Additionally, control measurements with DCM-doped LC droplets showed similar behavior. The present study focused on Nile Blue due to its high quantum yield and solubility in LC–water interfaces; future work may explore alternative, more photostable dyes to further validate system robustness.

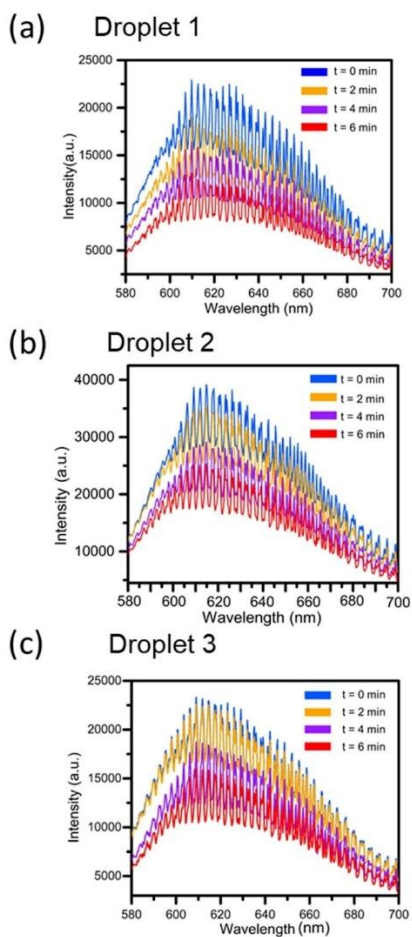


Figure 12. Time-dependent WGM spectra of three dye-doped liquid crystal microdroplets (Droplets 1–3) under continuous optical trapping. Spectra recorded at $t = 0, 2, 4,$ and 6 minutes show the gradual decrease in fluorescence intensity due to photobleaching while retaining the characteristic WGM structure.

S13. Characterisation of AuNPs with basic units of 100/200/400 nm with statistical data.

The basic unit sizes of 100, 200, and 400 nm refer to the nominal diameters of the individual gold nanoparticles used for cluster formation. Electron microscopy images were obtained by drop-casting the nanoparticle suspension onto a silicon substrate and allowing it to dry for several hours before imaging. After drying, the substrate was used for electron microscopy to visualise the nanoparticle assemblies.

We obtained nanoparticle clusters of various sizes, which may differ slightly from the morphologies formed under the conditions used in our optical-tweezers experiments, where the clusters remained dispersed in water. The provided images therefore represent the approximate size and morphology of the clusters used in our parking experiments for the 100, 200, and 400 nm basic unit nanoparticle sizes.

We have now included electron microscopy–based characterisation of these clusters, supplying rough estimates of their average diameters and the approximate number of particles per cluster.

Assumptions & method

Estimated cluster parameters for 100 nm nanoparticle cluster

- Individual particle diameter $d = 0.1 \mu\text{m}$ (100 nm).
- Area of one particle $A = \pi\left(\frac{d}{2}\right)^2 = \pi(0.05)^2 = 0.00785 \mu\text{m}^2$
- 2D effective packing fraction f (occupied area ratio) 0.7 (typical for clustered / partial packed aggregates).
- Estimated cluster area $A_{\text{cluster}} = (N)(A)/f$, where N = number of particles in cluster.
- Equivalent cluster diameter $D_{\text{eq}} = \left(\frac{4A_{\text{cluster}}}{\pi}\right)^{0.5}$.
- Morphology/particle counts estimated visually from the SEM images.

Panel	Morphology (Visual)	N (particles)	Projected area $A_{\text{cluster}} (\mu\text{m}^2)$	$D_{\text{eq}} (\mu\text{m})$
Left	Dense aggregate (layered)	37	$37 \times (0.00785)$ $= 0.29$	0.60
Middle	Partially compact/elongated	15	$15 \times (0.00785)$ $= 0.118$	0.38
Right	Dense aggregate (layered)	33	$33 \times (0.00785)$ $= 0.259$	0.57

Average number of particles in the cluster of 100 nm = $(37 + 15 + 33)/3 = 28.33$

SEM images of a cluster with a basic unit of 100 nm are given below:

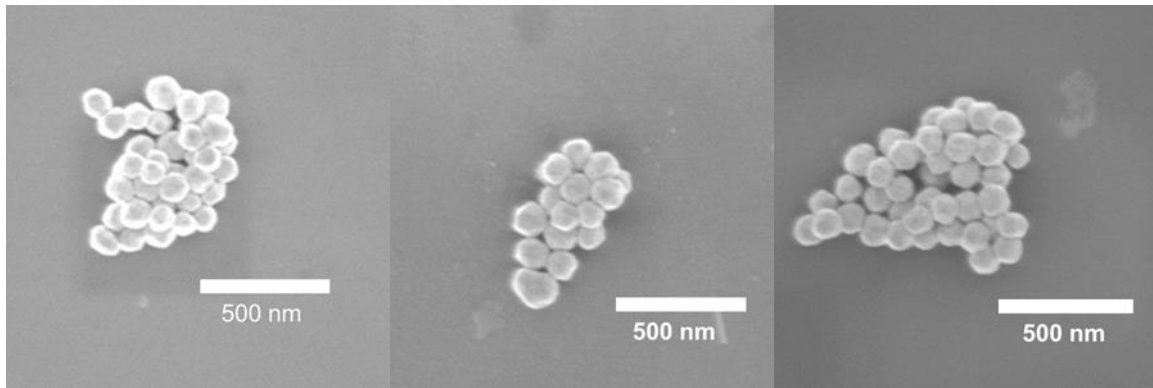


Figure 13. SEM images showing representative morphologies of gold nanoparticle clusters composed of spherical nanoparticles of 100 nm diameter. Scale bar: 500 nm.

Estimated cluster parameters for 200 nm nanoparticle cluster

- Individual particle diameter $d = 0.2 \mu\text{m}$ (200 nm).
- Area of one particle $A = \pi\left(\frac{d}{2}\right)^2 = \pi(0.1)^2 = 0.0314 \mu\text{m}^2$

Panel	Morphology (Visual)	N (particles)	Projected area $A_{\text{cluster}} (\mu\text{m}^2)$	$D_{\text{eq}} (\mu\text{m})$
Left	Partially compact/elongated (layered)	35	$35 \times (0.0314)$ $= 1.1$	1.18
Middle	Compact aggregate (layered)	18	$18 \times (0.0314)$ $= 0.565$	0.84
Right	Dense aggregate	30	$30 \times (0.0314)$ $= 0.942$	1.1

Average number of particles in the cluster of 200 nm = $(35 + 18 + 30)/3 = 27.66$

SEM images of a cluster with a basic unit of 200 nm are given below:

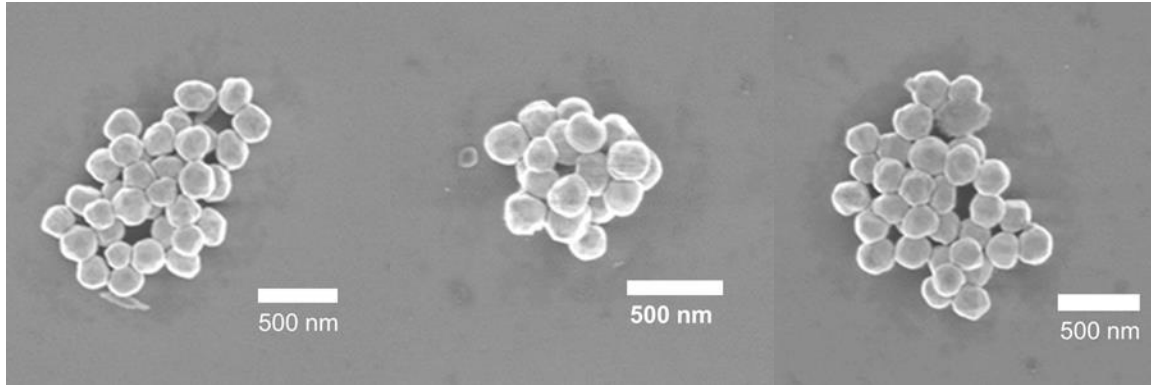


Figure 14. SEM images showing representative morphologies of gold nanoparticle clusters composed of spherical nanoparticles of 200 nm diameter. Scale bar: 500 nm.

Estimated cluster parameters for 400 nm nanoparticle cluster

- Individual particle diameter $d = 0.4 \mu\text{m}$ (400 nm).
- Area of one particle $A = \pi\left(\frac{d}{2}\right)^2 = \pi(0.2)^2 = 0.1256 \mu\text{m}^2$

Panel	Morphology (Visual)	N (particles)	Projected area $A_{\text{cluster}} (\mu\text{m}^2)$	$D_{eq} (\mu\text{m})$
Left	Branched cluster (Chain-like, open branching network)	26	$26 * (0.1256)$ $= 3.26$	2.03
Middle	Partially compact cluster (open branching)	76	$76 * (0.1256)$ $= 9.54$	3.48
Right	Dense cluster	31	$31 * (0.1256)$ $= 3.89$	2.22

Average number of particles in the cluster of 400 nm = $(26 + 76 + 31)/3 = 44.33$

SEM images of a cluster with a basic unit of 400 nm are given below:

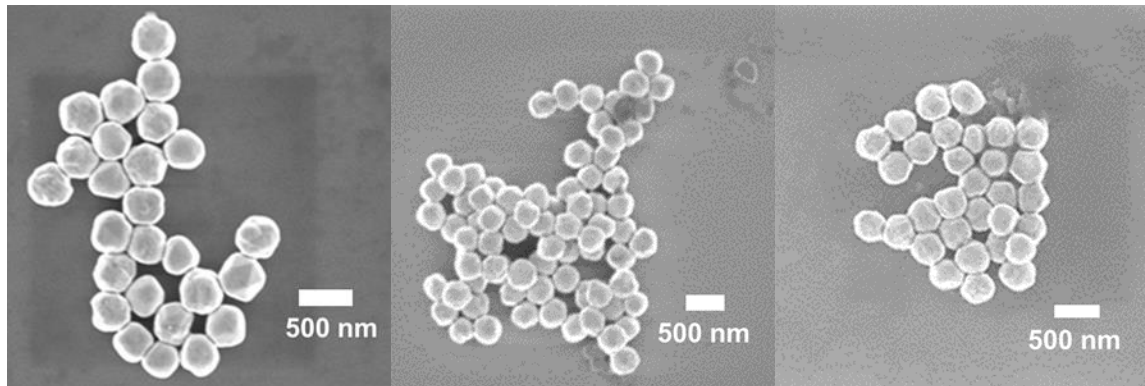


Figure 15. SEM images showing representative morphologies of gold nanoparticle clusters composed of spherical nanoparticles of 400 nm diameter. Scale bar: 500 nm.

S14. Table of plasmonic tuning observed in solid versus liquid crystal microresonator.

A quantitative comparison summarising the magnitude of plasmonic tuning observed in solid versus liquid crystal microresonators is provided in Table 1, clearly illustrating that the tunable shift achieved in our soft, reconfigurable droplet-based system exceeds that of solid microresonators by nearly two orders of magnitude, thereby highlighting the enhanced field–matter interaction and dynamic tunability enabled by optical trapping.

Table 1. Quantitative comparison of plasmonic-induced resonance shifts in microresonator systems

System type	Resonator diameter	Observed redshift (nm)	Reference
Solid microcavity (single nanodisk)	200 μm	0.011	Kim <i>et al.</i> [1]
Solid microcavity (double nanodisk)	200 μm	0.036	Kim <i>et al.</i> [1]
Dye-doped nematic LC microdroplet	$\sim 15\text{--}25 \mu\text{m}$	7.1	This work

References

- [1] W. Ahn, S. V. Boriskina, Y. Hong and B. M. Reinhard, *ACS Nano*, 2012, **6**, 951–960.
- [2] M. R. Gartia, S. Seo, J. Kim, T.-W. Chang, G. Bahl, M. Lu, G. L. Liu and J. G. Eden, *Sci. Rep.*, 2014, **4**, 6168.
- [3] Y. Kang, W. Lee, H. Ahn, D.-M. Shin, C.-S. Kim, J.-W. Oh, D. Kim and K. Kim, *Sci. Rep.*, 2017, **7**, 11737.
- [4] M. Humar, M. Ravnik, S. Pajk and I. Muševič, *Nat. Photonics*, 2009, **3**, 595–600.
- [5] J. A. Sofi, M. Mohiddon, N. Dutta and S. Dhara, *Phys. Rev. E*, 2017, **96**, 022702.
- [6] P. Anger, P. Bharadwaj and L. Novotny, *Phys. Rev. Lett.*, 2006, **96**, 113002.